JOTCS A
Journal of the Turkish Chemical Society
Section: A
Chemistry
TURKISH CHEMICAL SOCIETY

Voltammetric Determination of Trace Amounts of Lead with Novel Graphite/Bleaching Earth Modified Electrode

Elif Tüzün[1]*

[1] Istanbul University-Cerrahpaşa, Department of Chemistry, Istanbul, 34320, Türkiye.

Abstract: Modified composite electrodes have gained considerable interest in the detection of heavy metal ions due to their excellent sensitivity, selectivity, stability, and rapid response. Generally, these sensors consist of binder, conductive substance, and modifier. This study examined into the performance of a novel modified electrode that used a graphite–bleaching earth (BE-MCPE) composite performed while detecting trace amounts of Pb(II) using a differential pulse voltammetric technique (DPASV). In order to investigate the properties of BE-MCPE, we employed several analytical techniques, including SEM, SEM-EDX, FTIR, and XRD. These techniques were used to characterize the physical, chemical, and elemental properties of BE-MCPE, as well as its Pb(II) adsorption capacity, providing a comprehensive understanding of its composition and structure. The electrochemical results showed that the modified electrode demonstrated superior sensitivity and selectivity, in detecting Pb(II) ions, with a linear response range of 2.10^{-7} mol/L to 10.10^{-7} mol/L , limit of detection (LOD) of $4.89x10^{-8}$ mol/L, and limit of quantification (LOQ) of $1.63x10^{-7}$ mol/L. This novel modified electrode can achieve the sensitive detection of trace amounts of Pb(II) in a wide range of wastewater applications.

Keywords: Bleaching earth, Clay, Heavy metal, Modified electrode, Voltammetry.

Submitted: April 15, 2023. **Accepted:** June 19, 2023.

Cite this: Tüzün E. Voltammetric Determination of Trace Amounts of Lead with Novel Graphite/Bleaching Earth Modified Electrode. JOTCSA. 2023;10(3):659-70.

DOI: https://doi.org/10.18596/jotcsa.1283767

***Corresponding author's E-mail:** elif.tuzun@iuc.edu.tr

1. INTRODUCTION

The development of modified composite electrodes has gained considerable attention, particularly in the field of sensing heavy metal ions (1). The market for modified composite electrodes is growing rapidly in the field of heavy metal ion detection due to their exceptional stability, sensitivity, flexibilty, selectivity, wearability, and rapid response time. These sensors are highly significant in detecting trace amounts of heavy metal ions in a variety of industrial and environmental applications thanks to their unique properties (2). Human activities have resulted in the discharge of a large number of contaminants into the environment, which has had a detrimental impact on the environment (3). These heavy metals can accumulate through food chains, plants, water, air, and soil, which can have a major adverse effect on environments and living organisms (4–6). This problematic issue involves several dangerous and harmful metals, including iron, mercury, arsenic, silver, copper, nickel, cobalt, and zinc. These metals are known to be cumulative in nature, and their toxic effects can increase over time, making them particularly hazardous (7). Extremely dangerous environmental hazards including Pb(II) (5,8–10), Hg(II) (5,9), Cu(II) (9,11), and Cd(II) (5,9) can damage the liver, heart, bone, kidney, muscle, skin, teeth, and nervous system, among other organs in the body. Additionally, Pb(II) is a critical trace element for humans, but excessive amounts can accumulate in the body's tissues, leading to overdose and potentially fatal consequences such as renal damage. Therefore, it is crucial to monitor the concentration of these heavy metal ions carefully (12).

Nowadays, a number of methods have been suggested for the detection of heavy metal ions, including atomic emission spectroscopy (AES), inductively coupled plasma mass spectrometry (ICP-MS), atomic absorption spectroscopy (AAS) (13), etc. Currently, several methods such as ICP-MS (14), colorimetric method (15), AAS, near-infrared

spectroscopy (16), direct thermal release/electrothermal atomization atomic absorption spectrophotometric (ETA AAS) detection (17) and voltammetric method (18) have been proposed for detecting heavy metal ions.

The silver nanoparticles/silane grafted bentonite modified electrode investigated by Lalmalsawmi et al. demonstrated remarkable both sensitivity and selectivity for detecting a small quantity of Pb(II) in wastewater applications (19). Electrochemical sensing systems offer excellent advantages for detecting Pb(II) ions using modified glassy carbon electrode surface. For detecting contamination by heavy metals in both industrial and environmental situations, such a type of electrode may provide an efficient and economical solution. In another study, using linear scan anodic stripping voltammetry (LSASV) and cyclic voltammetry (CV), Jaber et al. investigated the selectivity of membrane filtration ceramic membranes fabricated from local clay against Pb(II) (20). The novelty of this study lies in the utilization of graphite-bleaching earth (BE-MCPE) composite as a novel modifier for the determination of trace amounts of Pb(II) using differential pulse anodic stripping voltammetry (DPASV). The graphite-bleaching earth composite working electrodes offer the advantages of simplicity, ease of preparation, and cost-effectiveness, while taking advantage of the reactivity and sensitivity of clay, making them suitable for routine analysis of Pb(II) in environmental medium. This study presents the high value of clay-modified electrodes in the perspective of ceramic membrane filtration for heavy metal ions, particularly Pb(II), in terms of efficiency. In order to investigate the properties of BE-MCPE, we employed several analytical techniques, including scanning electron microscopy (SEM), SEM combined with energy-dispersive X-ray spectroscopy (SEM-EDX), Fourier transform infrared spectroscopy (FTIR), and X-ray diffraction (XRD). These techniques were used to determine the physical, chemical, and elemental properties of BE-MCPE, as well as its Pb(II) adsorption capacity, providing a comprehensive understanding of its composition and structure. Using DPASV, our study examined the efficacy of a novel graphite-bleaching earth composite modified electrode for the selective detection of trace amounts of Pb(II). With a linear response range of 2.10^{-7} M to 10.10^{-7} M, LOD of $4.89x10^{-8}$ mol/L, and LOQ of $1.63x10^{-7}$ mol/L, the modified electrode demonstrated excellent sensitivity and selectivity, making it a promising solution for detecting Pb(II) in wastewater applications.

2. EXPERIMENTAL

2.1. Apparatus and Chemicals

The bleaching earth was collected from Edremit, Türkiye. The main component in bleaching earth, with a chemical formula of $Al_2O_3 4SiO_2 nH_2O$, is silicon dioxide. It is a very fine powder that can range from 57% to more, depending on the type (21). The clay material was manually ground with a mortar and pestle before being separated into various granular sizes with ASTM (American Society for Testing and Materials) specified sieves. The sieves were stacked on top of one another to collect around 4 sizes. The bleaching earth membrane supports were produced using fractions of a size in the 200–400 μm range. Lead(II) nitrate (≥ 99.0%), cadmium(II) nitrate (≥ 99.0%), mercury(II) nitrate (≥ 99.0%), and copper(II) nitrate (≥ 99.0%), were purchased from Sigma Aldrich Company. Graphite powder (particle size < 100μm) and spectroscopic-grade paraffin oil were procured from Fluka Company.

A Gamry (Inst.Ref.600 potentiostat/galvanostat) was used to regulate the current and voltage during electrochemical processes. A working electrode, a reference electrode, and a counter electrode makes up the 3-electrode configuration used. In this study, a BE-MCPE served as the working electrode. The counter electrode was Pt wire, and the reference electrode was a Ag/AgCl electrode in a 3 M KCl solution. The use of the reference and counter electrodes creates a stable baseline for comparison and result analysis, allowing for precise control and monitoring of the electrochemical reactions occurring on the BE-MCPE working electrode. The experiment was carried out with high-quality and precisely measured ingredients, increasing the likelihood of achieving exact and trustworthy results. The experiment used only analytical reagent grade chemicals. In addition, Millipore Direct-Q3 water, which has a high level of purity (18 Mega cm), was used to make all of the aqueous solutions for the experiment, reducing any sources of impurities or contaminants that might have an impact on the experiment's outcomes. It was necessary to use a buffer solution as a supporting electrolyte for the measurement of Pb(II) concentration. The buffer utilized was a 0.05 M NaOAc-HOAc solution with a pH of 4.75. The accuracy and precision of the data obtained depended heavily on selecting of this buffer solution. The buffer solution aids in preserving an electrochemical reaction's stable pH environment, ensuring that the reaction takes place under constant and dependable circumstances. In turn, this contributes to reducing experimental mistakes and improving the precision and clarity of the findings. A stock solution of Pb(II) ($1x10^{-3}$ M) was prepared from the corresponding analytical grade metal nitrate. The BE-MCPE was prepared by mixing 0.5 g of graphite, 0.3 g of BE, and 100 μL of paraffin oil by hand-mixing in a mortar, and then the sample was homogenized. The MCPE was pressed into the cavity of the electrode body, and the electrical contact was established with a Pt. The surface and functional groups of the synthesized BE-MCPE were analyzed using various techniques such as SEM (Model: Hitachi SU3500 T2), EDX (Model: Oxford XACT), FTIR (Model: Jasco 6800), and XRD (Rigaku Miniflex 600). By scanning the surface with an electron beam at a 15 kV acceleration voltage in vacuum, we were able to obtain SEM images of solid powder samples. To identify the functional groups contained in the material, 32 scans were recorded across a range of 4000-400 cm^{-1} to create the FTIR spectra of the samples. Additionally, the crystal structure and average crystallite size of the BE-MCPE were determined using the XRD method with Cu K_α radiation (conditions: 40 kV and 15 mA).

2.2. Procedure

10 mL of pH 4.75 NaOAc-HOAc buffer solution in the voltammetric cell was filled with the BE-MCPE. The electrode was standardized for 5 minutes with an open circuit in the blank solution. After that, differential pulse voltammograms of blank solutions with the standardized electrode were recorded in the potential range of -0.8 V to -0.4 V until a stable voltammetric background was obtained. The electrode was removed, cleaned with water, and placed inside a different voltammetry cell that contains 10 mL of Pb(II) preconcentration solution. The accumulation step was carried out at -0.7 V for a selected time while stirring the solution at 650 and 500 rpm. After an appropriate preconcentration step, the electrode was rinsed with deionized water. Reduced lead was stripped from the electrode surface during the potential sweep from -0.8 V to -0.4 V, and well-defined stripping peaks were obtained between -0.54 V and -0.525 V, depending on the metal concentrations In Figure 1, the schematic experimental procedure is given.

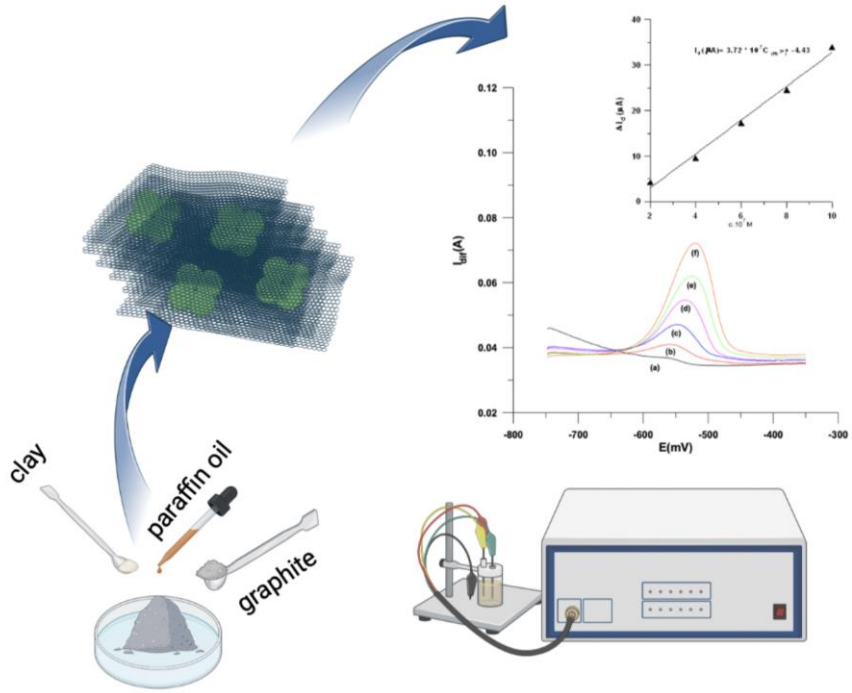

Figure 1: The schematic experimental procedure

3. RESULTS AND DISCUSSION

3.1. Characterization of Materials

FTIR analysis revealed characteristic peaks of functional groups for BE, BE-MCPE, and BE-MCPE /Pb. The technique was also utilized to illuminate the interactions between BE-MCPE and Pb(II) ions. In Figure 2 (a), the FTIR spectra of BE showed major characteristic peaks at about 3624, 3410, 1638, 1425, 1112,984, and 790 cm^{-1} which are attributed to the vibrations of O–H, stretching, O–H, stretching, –C=O, SiO, SiO, δAlAlOH, and silica, respectively. In Figure 2 (b), the FTIR spectra of BE-MCPE showed major characteristic peaks at about 3624, 2920, 2851, 1630, 1457, 1114, and 970 cm^{-1} which are attributed to the vibrations of O–H, stretching, –CH symmetric, –CH asymmetric, –C=O, SiO, SiO, and δAlAlOH, respectively. In Figure 2 (c), the FTIR spectra of BE-MCPE /Pb showed major characteristic peaks at about 2920, 2851, 1356, and 970 cm^{-1} which are attributed to the vibrations of –CH symmetric, –CH asymmetric, SiO, and δAlAlOH, respectively. The result is in good agreement with other literature reports (21–23). The absorption spectrum showed notable changes following the adsorption of Pb (Figure 2). Specifically, the peak corresponding to ν (−OH) displayed a shift to 3619 cm^{-1}, while the peak associated with ν (C=O) shifted to 1630 cm^{-1}. Additionally, the intensity of the peak related to ν (C=O) significantly decreased, and the peak of 1638 cm^{-1} underwent a shift to 1457 cm^{-1} and decreased noticeably in intensity.

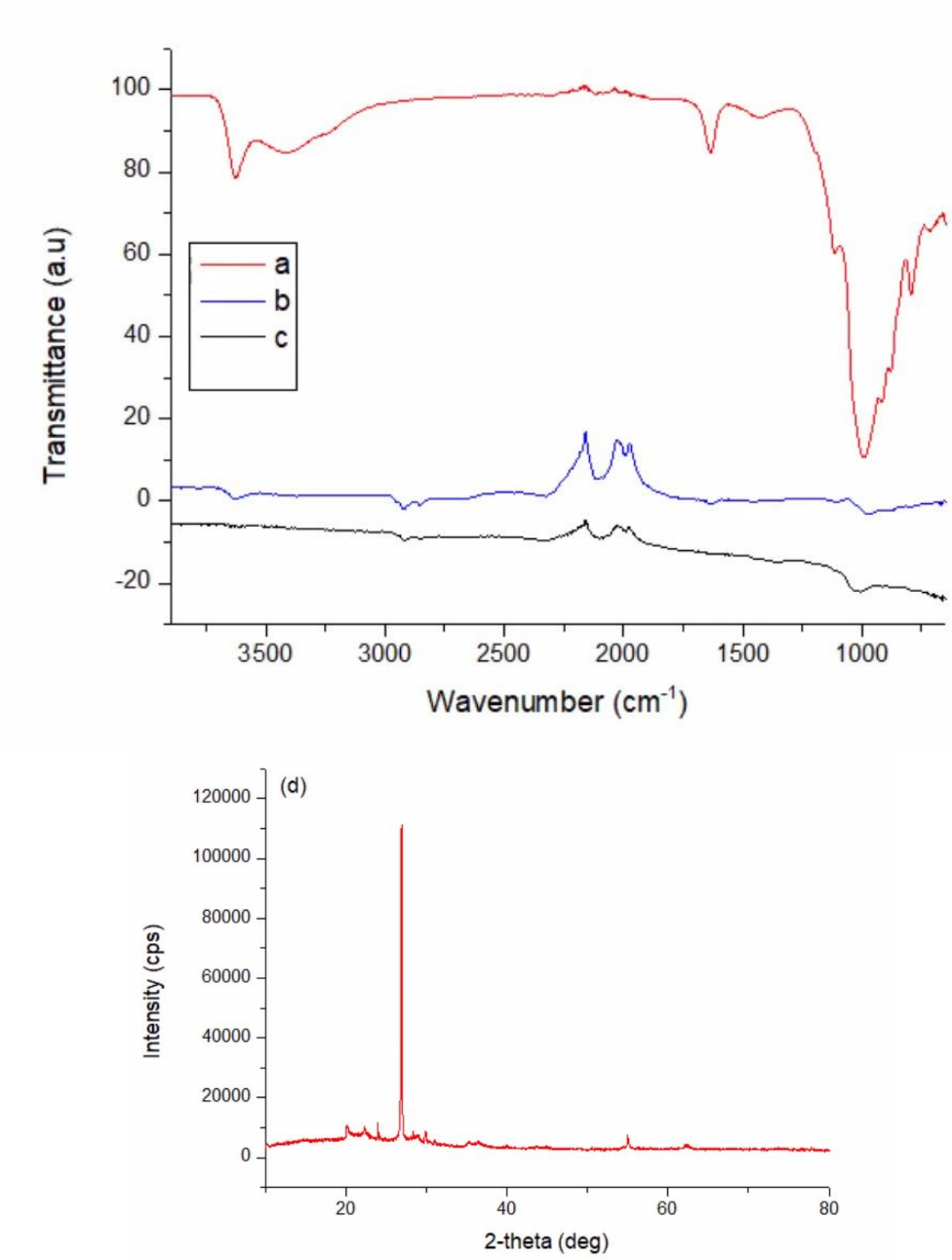

Figure 2: FTIR spectra of (a) BE, (b) BE-MCPE, (c) BE-MCPE/Pb, and (d) XRD graph of BE-MCPE.

In this study, SEM mapping and EDX data were utilized to analyze the BE-MCPE's composition and distribution, while also investigating its surficial properties. Figure 3 displays SEM images of samples (a) BE, (b) BE-MCPE's, and (c) BE-MCPE /Pb(II)'s. The SEM analysis of the BE showed that the sample contained particles with a plate-like morphology, indicating the presence of layered clay structures (24). These structures were thin and flat, similar to sheets or small plates stacked on top of each other. The SEM image of the BE-MCPE composite showed a morphology that resembled the distribution of several individual graphene layers gathering and folding into a layered clay structure during the formation of the composite. In this study, the elemental composition of the BE-MCPE/Pb(II) (Figure 3.d) was investigated using EDX analysis, and the obtained results are presented in Table 2. The results showed the presence of various elements, including silisium (27.72%), calcium (1.74%) lead (13.32%), iron (3.24%), potasium (1.00%), magnesium (1.12%), aluminum (8.83%), and oxygen (43.03%) in the sample. After adsorption, it was observed that the distance between the folded layers was partially closed and Pb(II) was dispersed on the structure. The SEM-EDX results confirmed this interaction. These images provide evidence of the successful formation of adsorption.

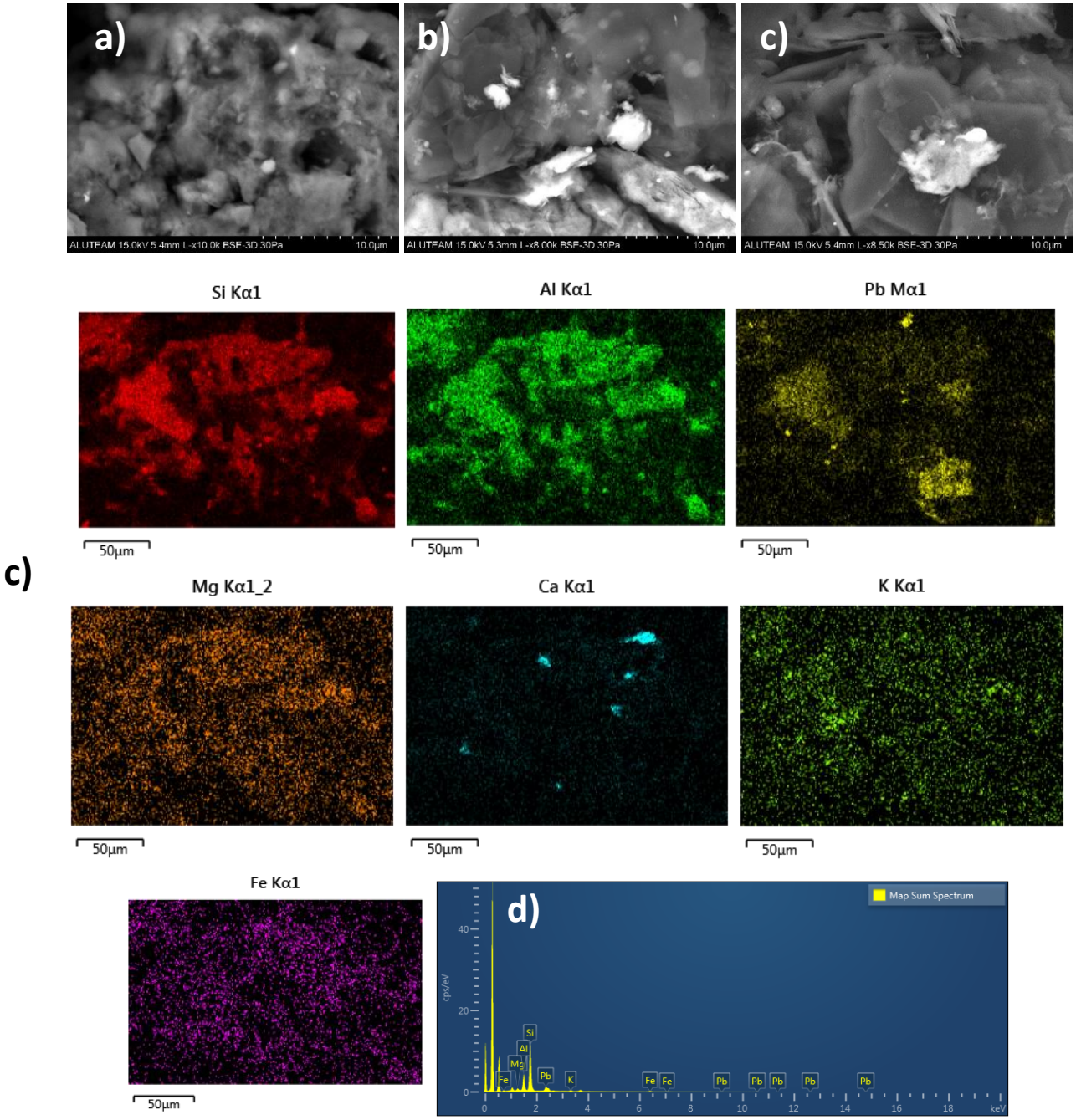

Figure 3: SEM images of (a) BE, (b) BE-MCPE, (c) BE-MCPE /Pb(II), (d) SEM mapping of BE-MCPE /Pb(II), and SEM-EDX graph of BE-MCPE /Pb(II).

The crystalline size of BE-MCPE was calculated using X-ray powder diffraction (XRD) analysis. The XRD pattern of the prepared BE-MCPE is presented in Figure 2 (d), which displays distinct peaks at $2\theta = 26.99^{o}$, 40.04^{o} and 66.76^{o} corresponding to JCPDS file 00-038-0449. Using the Scherrer Equation, the crystalline sizes of the BE-MCPE was found to be 17 nm, as depicted in Figure 3. These results were consistent with the SEM, and were in agreement with the findings of a related study (25). The formula for Debye-Scherrer equation (26) is:

$$n\lambda = 2d \sin \theta \qquad (3.1)$$

where the variable "n" represents the diffraction peak order, "λ" denotes the wavelength of X-rays applied, "d" stands for the interplanar spacing of the crystal lattice, and "θ" represents the angle of diffraction.

The calibration graphs of current of versus Pb(II) concentration in the range of (2-10)x10^{-7} mol/L for an accumulation time of 5 minutes and a potential of -0.7 V and stirring rates of 500 rpm and 650 rpm at BE-MCPE are shown in Figures 4 and 5, respectively. Linear relationships were observed in the calibration graphs in the range of (2-10)x10^{-7} mol/L for both mixing speeds. The detection limits and straight-line equations for all of the results are provided in Table 1.

The effect of mixing speed on BE-MCPE performance was investigated in the range of (2-10)x10^{-7} mol/L. The signals for Pb(II) increased with increasing mixing speed of the enrichment solution up to 500 and/or 650 rpm and then slowed down. Higher mixing speeds resulted in lower signals due to surficial degeneration. Therefore, the stirring speed was optimized at 500 rpm and 650 rpm for all voltammetric experiments.

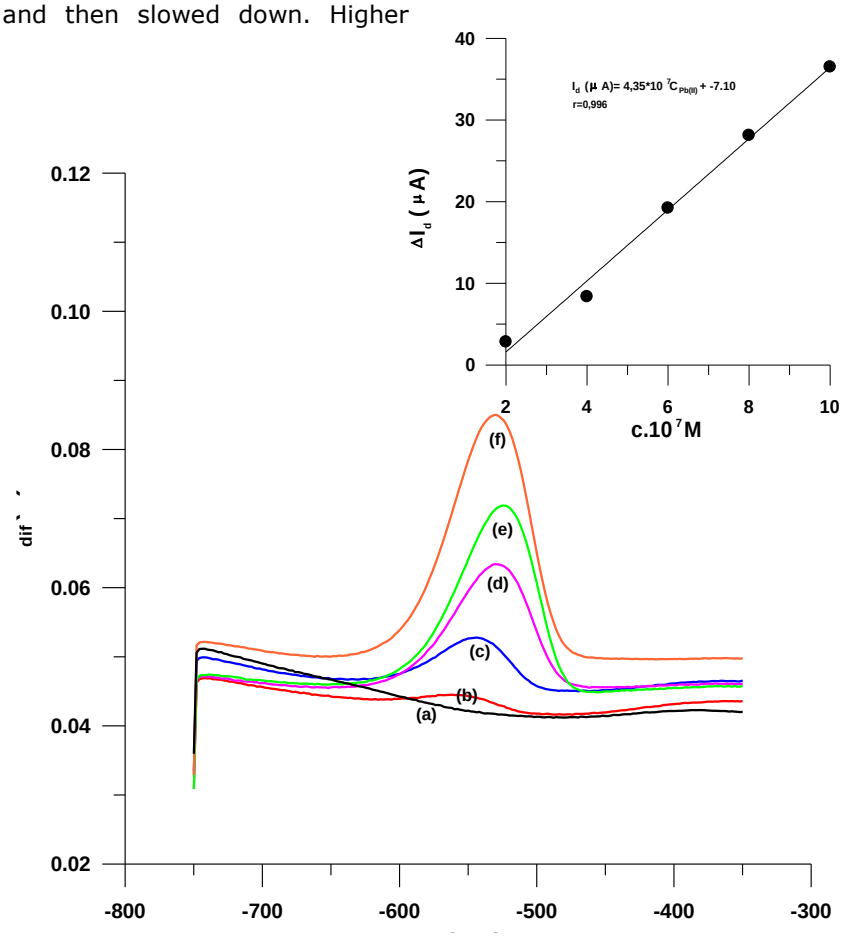

Figure 4: DPAS voltammograms and calibration graph of current vs Pb(II) concentrations (a) Blank, (b) 2.10^{-7} mol/L Pb(II), (c) 4.10^{-7} mol/L Pb(II), (d) 6.10^{-7} mol/L Pb(II), (e) 8.10^{-7} mol/L Pb(II), (f) 10.10^{-7} mol/L Pb(II) (-0.7 V, 5 min, 500 rpm)

Table 1: Comparison of analytical performance measurements of BE-MCPE with different modified electrodes in the literature for the determination of heavy metal ions.

Electrode	Technique	LOD	Ref.
N^1-hydroxy-N^1,N^2-diphenylbenzamidine- Carbon paste electrode(CPE)	SWASV	0.0094 nm (Pb)	(27)
Ion-imprinted polymers- CPE	DPASV	0.99 mg /L (Pb)	(28)
(Ag)/ (Au)-(NP)glassy carbon electrode(GCE)	DPASV	0.03×10^{-2} µg /L (Pb)	(29)
Bi oxycarbide /GCE	DPASV	3.97 µg /L (Pb) 4.24 µg /L (Cd)	(30)
Hg-Bi/ poly(1,2-diaminoanthraquinone)/GCE	ASV	0.069 µg /L (Pb) 0.195 µg /L (Cd) 0.169 µg /L (Zn)	(31)
Bi/carboxyphenyl-modified GCE	SWASV	10 µg /L (Pb) 25 µg /L (Cd)	(32)
Graphene quantum dots and Nafion modified GCE	SWASV	8.49 µg /L (Pb) 11.30 µg /L (Cd)	(33)
Ag nanoparticles-silane grafted bentonite material	DPASV	0.88 µg /L (Pb) 0.79 µg /L (Cd)	(19)
BE-MCPE	DPASV	4.89x10^{-8} mol /L (500 rpm)(Pb) 3.57x10^{-8} mol /L (650 rpm)(Pb)	This work

It is shown in Table 1 that the BE-MCPE sensor exhibits excellent sensitivity and selectivity for the detection of heavy metal ions, especially Pb(II), making it a promising tool for trace-level monitoring in various environmental applications. Table 1 also compares the analytical performance measurements of the BE-MCPE with other modified electrodes reported in the literature.

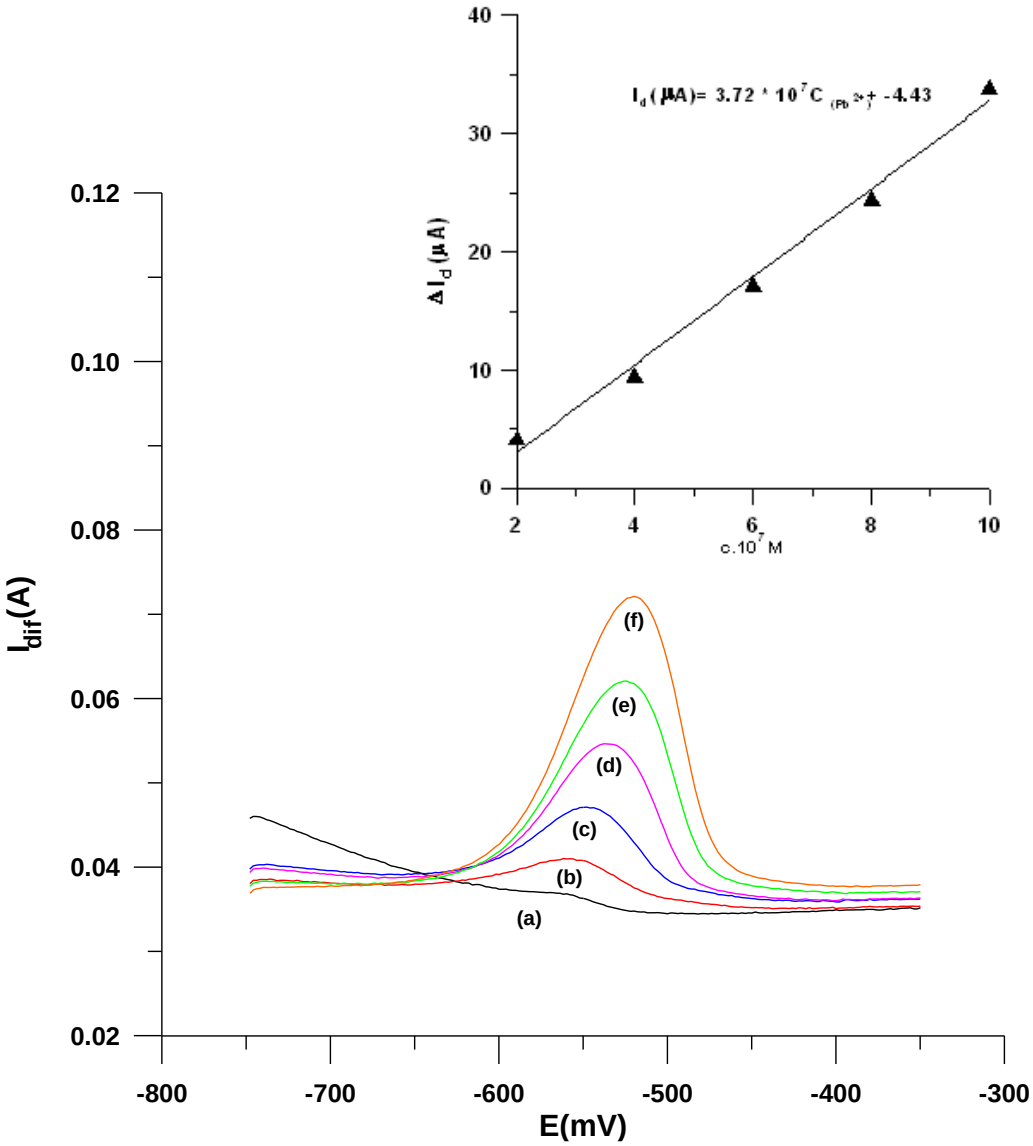

Figure 5: DPAS voltammograms and calibration graph of current vs Pb(II) concentrations (a) Blank (b) 2.10^{-7} mol/L Pb(II) (c) 4.10^{-7} mol/L Pb(II) (d) 6.10^{-7} mol/L Pb(II) (e) 8.10^{-7} mol/L Pb(II) (f) 10.10^{-7} mol/L Pb(II) (-0.7 V, 5 min, 650 rpm)

It is suggested that the reduction and oxidation of Pb(II) solution on the BE-MCPE surface occurs in a three-step reaction process, as described below (Equation 3.2-3.4), based on the results of this study and other relevant investigations (27).

(Pb^{2+}) (aq) + BE-MCPE → $(Pb^{2+}$ - BE-MCPE) complex (3.2)

$(Pb^{2+}$ - BE-MCPE) complex $+2e^-$ → (Pb – BE-MCPE) complex (3.3)

(Pb – BE-MCPE) complex - $2e^-$ → (Pb^{2+}) (aq)/electrode + BE-MCPE (3.4)

3.2. Optimization of the Solution pH

The effect of pH on the DPASV response was studied in 5.10^{-7} mol/L Pb(II) solution with a settling time of 5 minutes. Electrode current was measured at a potential of -0.7 V and stirring rate of 500 rpm at pH values ranging from 1.0 – 8.0 on BE-MCPE. The maximum peak current and peak potential were obtained at pH 5.20 (see Figure 6). The peak current and peak potential gradually increased with increasing pH of the pre-enrichment solution in the acidic range, reaching a maximum at pH 5.20, and then decreased sharply until reaching pH 8.01.

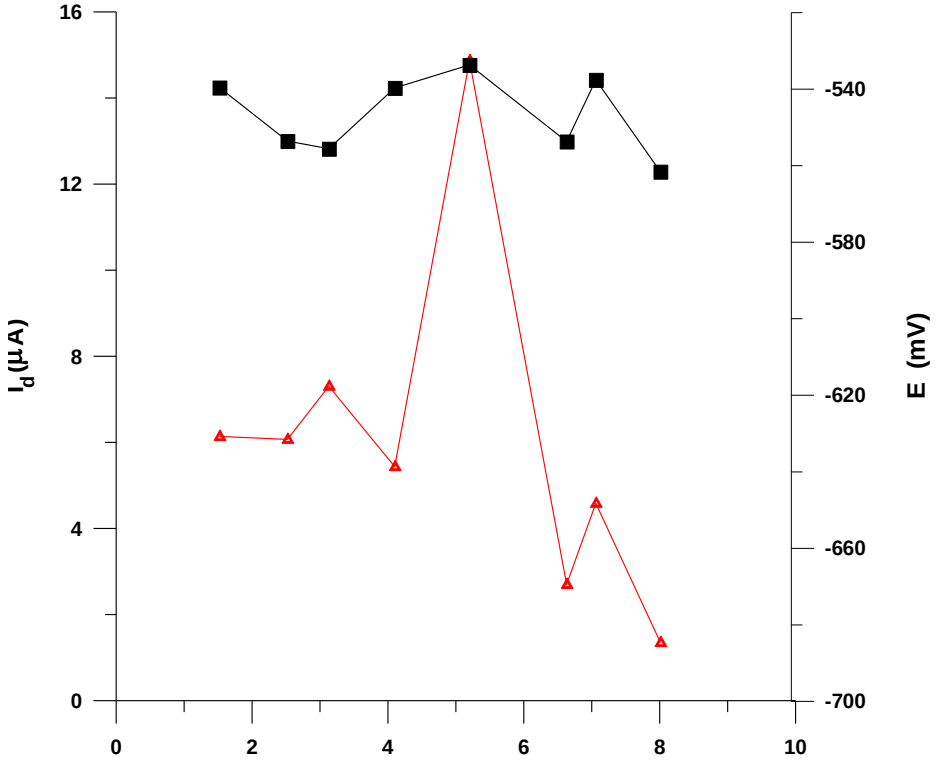

Figure 6: The influence of pH on diffusion currents and peak potentials of Pb(II) ion a) I_d vs pH b) E vs pH.

3.3. Simultaneous Determination of Heavy Metals in Binary Solutions

The effect of interference of some metal ions (Cd^{2+}, Hg^{2+} and Cu^{2+}) on the selectivity of BE-MCPE was also investigated. The tolerable concentrations of foreign species in the standard solution of Pb(II) concentration in the range of (2-10)x10^{-7} mol/L were as high as a 10-fold excess. When determining Pb(II), the interferences from Cu(II) and Hg(II) exhibited different behaviors regarding selectivity for Pb(II) ions. The shape of peak signals of Pb(II) ion concentration in the range of (2-10)x10^{-7} mol/L were not linear in the presence of 2x10^{-6} mol/L Cd(II) and Cu(II) ions (Figure 7) but were linear in presence of 2x10^{-6} mol/L Cd(II) and Hg(II) ions (Figure 8). The results showed that a 10 fold excess of Cu(II) ,Cd(II) and Hg(II) does not result in an interference in the determination of Pb(II). As a result, the carbon paste electrode modified with bleaching earth was proven to be a simple and selective sensor for the determination of Pb(II) in the trace concentration range.

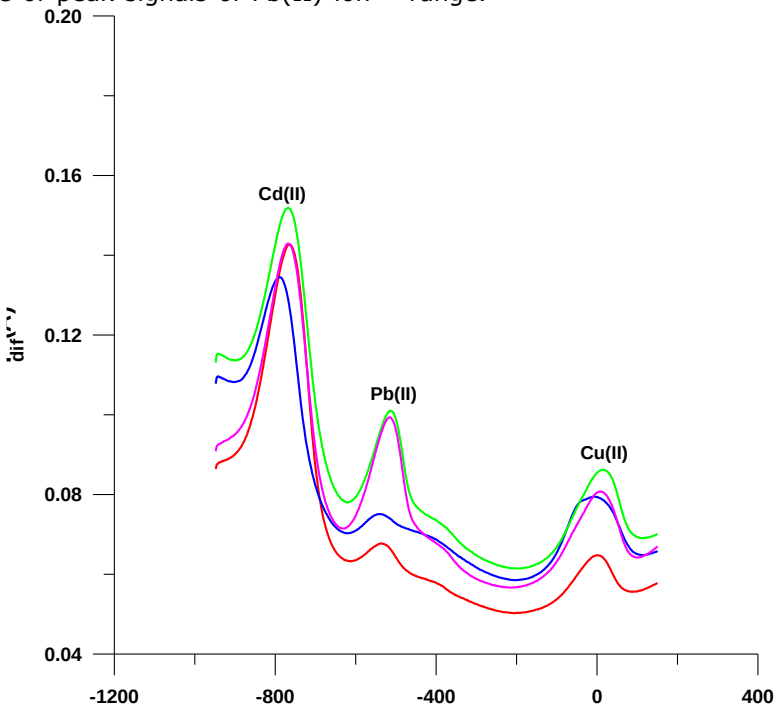

Figure 7: The effect of interference of some metal ions (Cd^{2+} and Cu^{2+}) on the Pb(II) ion selectivity of BE-MCPE.

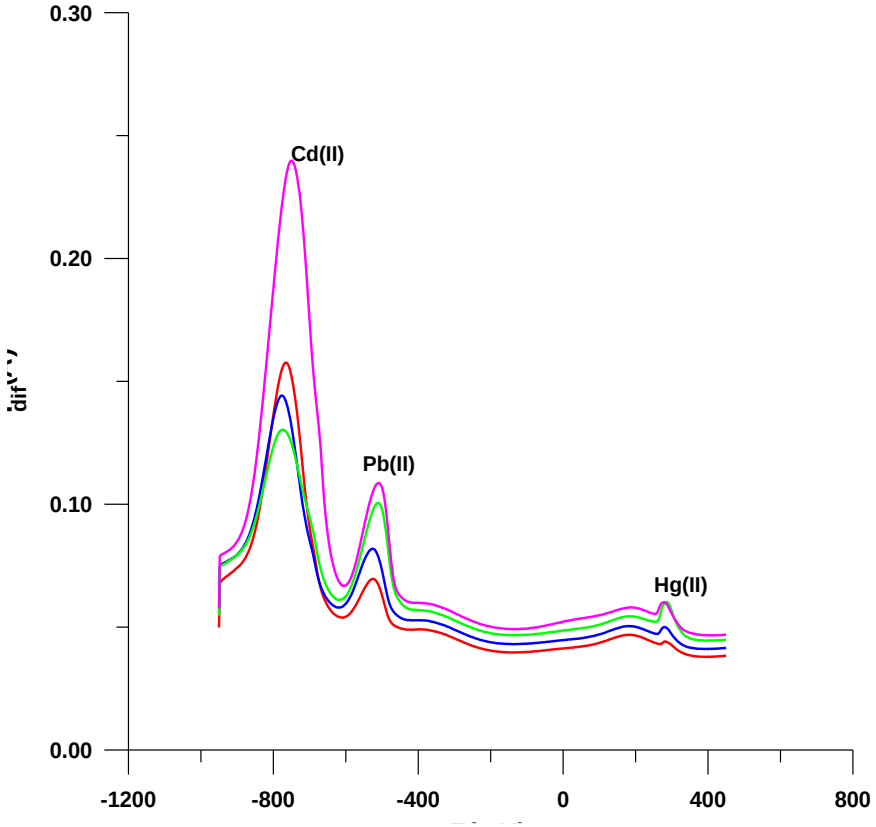

Figure 8: The effect of interference of some metal ions (Cd^{2+} and Hg^{2+}) on the Pb(II) ion selectivity of BE-MCPE.(34)

4. CONCLUSION

In conclusion, the use of modified composite electrodes has proven to be an effective approach for detecting heavy metal ions in wastewater applications. The novel (BE-MCPE) composite electrode, studied here, demonstrated excellent sensitivity, selectivity, stability, and rapid response in detecting trace amounts of Pb(II) using a differential pulse voltammetry technique. The utilization of SEM, SEM-EDX, FTIR, and XRD techniques allowed for a thorough investigation of the features of BE-MCPE. Through the use of these techniques, we were able to explore the physical, chemical, and elemental properties of BE-MCPE, as well as its Pb(II) adsorption capacity. According to the electrochemical results, the linear response range was between 2.10^{-7} mol/L and 10.10^{-7} mol/L, with a (LOD) of 4.89×10^{-8} mol/L and a (LOQ) of 1.63×10^{-7} mol/L. This modified electrode therefore has the potential to be employed as a reliable and successful tool for observing and identifying small amounts of Pb(II) in a variety of wastewater treatment applications.

5. CONFLICT OF INTEREST

I declare that there is no conflict of interest related to this work. Furthermore, the author confirms that the paper is not under consideration by any other journal and has not been published previously.

6. REFERENCES

1. Wu Q, Bi H-M, Han X-J. Research Progress of Electrochemical Detection of Heavy Metal Ions. Chinese J Anal Chem [Internet]. 2021 Mar 1;49(3):330–40. Available from: <URL>.

2. Falina S, Syamsul M, Rhaffor NA, Sal Hamid S, Mohamed Zain KA, Abd Manaf A, et al. Ten Years Progress of Electrical Detection of Heavy Metal Ions (HMIs) Using Various Field-Effect Transistor (FET) Nanosensors: A Review. Biosensors [Internet]. 2021 Nov 25;11(12):478. Available from: <URL>.

3. Kumar V, Agrawal S, Bhat SA, Américo-Pinheiro JHP, Shahi SK, Kumar S. Environmental impact, health hazards, and plant-microbes synergism in remediation of emerging contaminants. Clean Chem Eng [Internet]. 2022 Jun;2:100030. Available from: <URL>.

4. Mitra S, Chakraborty AJ, Tareq AM, Emran T Bin, Nainu F, Khusro A, et al. Impact of heavy metals on the environment and human health: Novel therapeutic insights to counter the toxicity. J King Saud Univ - Sci [Internet]. 2022 Apr 1;34(3):101865. Available from: <URL>.

5. Balali-Mood M, Naseri K, Tahergorabi Z, Khazdair MR, Sadeghi M. Toxic Mechanisms of Five Heavy Metals: Mercury, Lead, Chromium, Cadmium, and Arsenic. Front Pharmacol [Internet]. 2021 Apr 13;12:643972. Available from: <URL>.

6. İlhan Ceylan B. Oxovanadium(IV) and Nickel(II) complexes obtained from 2,2′-dihydroxybenzophenone-S-methyl-thiosemicarbazone: Synthesis, characterization, electrochemistry, and antioxidant capability. Inorganica Chim Acta [Internet]. 2021 Mar 1;517:120186. Available from: <URL>.

7. Ahmad W, Alharthy RD, Zubair M, Ahmed M, Hameed A, Rafique S. Toxic and heavy metals contamination assessment in soil and water to evaluate human health risk. Sci Rep [Internet]. 2021 Aug 20;11(1):17006. Available from: <URL>.

8. Collin MS, Venkatraman SK, Vijayakumar N, Kanimozhi V, Arbaaz SM, Stacey RGS, et al. Bioaccumulation of lead (Pb) and its effects on human: A review. J Hazard Mater Adv [Internet]. 2022 Aug 1;7:100094. Available from: <URL>.

9. Penticoff HB, Fortin JS. Toxic/metabolic diseases of the nervous system. In: Neurobiology of Brain Disorders (Second Edition): Biological Basis of Neurological and Psychiatric Disorders [Internet]. Elsevier; 2023. p. 379–401. Available from: <URL>.

10. Romero-Estévez D, Yánez-Jácome GS, Navarrete H. Non-essential metal contamination in Ecuadorian agricultural production: A critical review. J Food Compos Anal [Internet]. 2023 Jan 1;115:104932. Available from: <URL>.

11. Jomova K, Makova M, Alomar SY, Alwasel SH, Nepovimova E, Kuca K, et al. Essential metals in health and disease. Chem Biol Interact [Internet]. 2022 Nov 1;367:110173. Available from: <URL>.

12. Li G, Qi X, Zhang G, Wang S, Li K, Wu J, et al. Low-cost voltammetric sensors for robust determination of toxic Cd(II) and Pb(II) in environment and food based on shuttle-like α-Fe2O3 nanoparticles decorated β-Bi2O3 microspheres. Microchem J [Internet]. 2022 Aug 1;179:107515. Available from: <URL>.

13. Mohammed H, Sadeek S, Mahmoud AR, Zaky D. Comparison of AAS, EDXRF, ICP-MS and INAA performance for determination of selected heavy metals in HFO ashes. Microchem J [Internet]. 2016 Sep 1;128:1–6. Available from: <URL>.

14. Fei J, Wu X, Sun Y, Zhao L, Min H, Cui X, et al. Preparation of a novel amino functionalized ion-imprinted hybrid monolithic column for the selective extraction of trace copper followed by ICP-MS detection. Anal Chim Acta [Internet]. 2021 Jun 1;1162:338477. Available from: <URL>.

15. Geleta GS. A colorimetric aptasensor based on two dimensional (2D) nanomaterial and gold nanoparticles for detection of toxic heavy metal ions: A review. Food Chem Adv [Internet]. 2023 Oct 1;2:100184. Available from: <URL>.

16. Jiang H, Lin H, Lin J, Yao-Say Solomon Adade S, Chen Q, Xue Z, et al. Non-destructive detection of multi-component heavy metals in corn oil using nano-modified colorimetric sensor combined with near-infrared spectroscopy. Food Control [Internet]. 2022 Mar 1;133:108640. Available from: <URL>.

17. Volynkin SS, Demakov PA, Shuvaeva O V., Kovalenko KA. Metal-organic framework application for mercury speciation using solid phase extraction followed by direct thermal release–electrothermal atomization atomic absorption spectrophotometric detection (ETA AAS). Anal Chim Acta [Internet]. 2021 Sep 8;1177:338795. Available from: <URL>.

18. Phan TTT, Nguyen TD, Lee JS. Vacuum plasma treatment on carbon nanoparticles for highly sensitive square wave voltammetric sensor of heavy metal ions. Synth Met [Internet]. 2022 Dec 1;291:117203. Available from: <URL>.

19. Lalmalsawmi J, Sarikokba, Tiwari D, Kim D-J. Simultaneous detection of Cd^{2+} and Pb^{2+} by differential pulse anodic stripping voltammetry: Use of highly efficient novel Ag0(NPs) decorated silane grafted bentonite material. J Electroanal Chem [Internet]. 2022 Aug 1;918:116490. Available from: <URL>.

20. Jaber L, Elgamouz A, Kawde A-N. An insight to the filtration mechanism of Pb(II) at the surface of a clay ceramic membrane through its preconcentration at the surface of a graphite/clay composite working electrode. Arab J Chem [Internet]. 2022 Dec 1;15(12):104303. Available from: <URL>.

21. Alabarse FG, Conceição RV, Balzaretti NM, Schenato F, Xavier AM. In-situ FTIR analyses of bentonite under high-pressure. Appl Clay Sci [Internet]. 2011 Jan 1;51(1–2):202–8. Available from: <URL>.

22. Shi W, Wang Z, Li F, Xu Y, Chen X. Multilayer adsorption of lead (Pb) and fulvic acid by Chlorella pyrenoidosa: Mechanism and impact of environmental factors. Chemosphere [Internet]. 2023 Jul 1;329:138596. Available from: <URL>.

23. Jin G, Gu P, Qin L, Li K, Guan Y, Su H. Preparation of manganese-oxides-coated magnetic microcrystalline cellulose via KMnO4 modification: Improving the counts of the acid groups and adsorption efficiency for Pb(II). Int J Biol Macromol [Internet]. 2023 Jun 1;239:124277. Available from: <URL>.

24. Neelaveni M, Santhana Krishnan P, Ramya R, Sonia Theres G, Shanthi K. Montmorillonite/graphene oxide nanocomposite as superior adsorbent for the adsorption of Rhodamine B and Nickel ion in binary system. Adv Powder Technol [Internet]. 2019 Mar 1;30(3):596–609. Available from: <URL>.

25. Huang H, Yi D, Lu Y, Wu X, Bai Y, Meng X, et al. Study on the adsorption behavior and mechanism of dimethyl sulfide on silver modified bentonite by in situ FTIR and temperature-programmed desorption. Chem Eng J [Internet]. 2013 Jun;225:447–55. Available from: <URL>.

26. Debye P. Zerstreuung von Röntgenstrahlen. Ann

Phys [Internet]. 1915;351(6):809–23. Available from: <URL>.

27. Tesfaye E, Chandravanshi BS, Negash N, Tessema M. A new modified carbon paste electrode using N1-hydroxy-N1,N2-diphenylbenzamidine for the square wave anodic stripping voltammetric determination of Pb(II) in environmental samples. Sens Bio-Sensing Res [Internet]. 2022 Dec;38:100520. Available from: <URL>.

28. Rebolledo-Perales LE, Álvarez Romero GA, Ibarra I, Galán-Vidal CA, Flores-Aguilar JF, Pérez-Silva I. Quantitative Analysis of Pb(II) Based on Differential Pulse Anodic Stripping Voltammetry and IIP-Carbon Paste Electrodes. J Electrochem Soc [Internet]. 2022 May 1;169(5):057504. Available from: <URL>.

29. Yadav R, Berlina AN, Zherdev A V., Gaur MS, Dzantiev BB. Rapid and selective electrochemical detection of Pb^{2+} ions using aptamer-conjugated alloy nanoparticles. SN Appl Sci [Internet]. 2020 Dec 25;2(12):2077. Available from: <URL>.

30. Zhang Y, Li C, Su Y, Mu W, Han X. Simultaneous detection of trace Cd(II) and Pb(II) by differential pulse anodic stripping voltammetry using a bismuth oxycarbide/nafion electrode. Inorg Chem Commun [Internet]. 2020 Jan;111:107672. Available from: <URL>.

31. Hassan KM, Gaber SE, Altahan MF, Azzem MA. Single and simultaneous voltammetric sensing of lead(II), cadmium(II) and zinc(II) using a bimetallic Hg-Bi supported on poly(1,2-diaminoanthraquinone)/glassy carbon modified electrode. Sens Bio-Sensing Res [Internet]. 2020 Aug;29:100369. Available from: <URL>.

32. Phal S, Nguyễn H, Berisha A, Tesfalidet S. In situ Bi/carboxyphenyl-modified glassy carbon electrode as a sensor platform for detection of Cd^{2+} and Pb^{2+} using square wave anodic stripping voltammetry. Sens Bio-Sensing Res [Internet]. 2021 Dec;34:100455. Available from: <URL>.

33. Pizarro J, Segura R, Tapia D, Navarro F, Fuenzalida F, Jesús Aguirre M. Inexpensive and green electrochemical sensor for the determination of Cd(II) and Pb(II) by square wave anodic stripping voltammetry in bivalve mollusks. Food Chem [Internet]. 2020 Aug;321:126682. Available from: <URL>.

34. Munir A, Shah A, Nisar J, Ashiq MN, Akhter MS, Shah AH. Selective and simultaneous detection of Zn^{2+}, Cd^{2+}, Pb^{2+}, Cu^{2+}, Hg^{2+} and Sr^{2+} using surfactant modified electrochemical sensors. Electrochim Acta [Internet]. 2019 Nov 10;323:134592. Available from: <URL>.